Petroleum Science 20 (2023) 3210–3222

Contents lists available at ScienceDirect

Petroleum Science

journal homepage: www.keaipublishing.com/en/journals/petroleum-science

Original Paper

Prediction of the viscosity of natural gas at high temperature and high pressure using free-volume theory and entropy scaling

Wei Xiong [a, *], Lie-Hui Zhang [a], Yu-Long Zhao [a, **], Qiu-Yun Hu [b], Ye Tian [a], Xiao He [c], Rui-Han Zhang [a], Tao Zhang [a]

[a] National Key Laboratory of Oil and Gas Reservoir Geology and Exploitation, Southwest Petroleum University, Chengdu, Sichuan, 610500, China
[b] Engineering Technology Research Institute, Southwest Oil and Gas Field Company, Chengdu, Sichuan, 610031, China
[c] PetroChina Southwest Oil & Gasfield Company, Chengdu, Sichuan, 610051, China

ARTICLE INFO

Article history:
Received 18 August 2022
Received in revised form
18 November 2022
Accepted 16 March 2023
Available online 17 March 2023

Edited by Jia-Jia Fei

Keywords:
Viscosity
Friction theory
Free volume theory
Entropy scaling
PC-SAFT Equation of state

ABSTRACT

Eighteen models based on two equations of state (EoS), three viscosity models, and four mixing rules were constructed to predict the viscosities of natural gases at high temperature and high pressure (HTHP) conditions. For pure substances, the parameters of free volume (FV) and entropy scaling (ES) models were found to scale with molecular weight, which indicates that the ordered behavior of parameters of Peng-Robinson (PR) and Perturbed-Chain Statistical Associating Fluid Theory (PC-SAFT) propagates to the behavior of parameters of viscosity model. Predicting the viscosities of natural gases showed that the FV and ES models respectively combined with MIX4 and MIX2 mixing rules produced the best accuracy. Moreover, the FV models were more accurate for predicting the viscosities of natural gases than ES models at HTHP conditions, while the ES models were superior to PRFT models. The average absolute relative deviations of the best accurate three models, i.e., PC-SAFT-FV-MIX4, tPR-FV-MIX4, and PC-SAFT-ES-MIX2, were 5.66%, 6.27%, and 6.50%, respectively, which was available for industrial production. Compared with the existing industrial models (corresponding states theory and LBC), the proposed three models were more accurate for modeling the viscosity of natural gas, including gas condensate.

1. Introduction

Correct predictions of phase behavior and viscosities of natural gases are very important for the design of natural gas processes (Tian et al., 2019; Mohagheghian et al., 2020; Xiong et al., 2020, 2021a; Zhang et al., 2021). The components of natural gases include *n*-alkanes, carbon dioxide (CO_2), hydrogen sulfide (H_2S), and nitrogen (N_2) (Zhang et al., 2020; Wei et al., 2021; Guo et al., 2022). The Peng-Robinson (PR) and Perturbed−Chain Statistical Associating Fluid Theory (PC-SAFT) equations of state (EoS) are usually used for phase equilibrium and viscosity modeling of natural gases (Bian et al., 2019; Jaubert et al., 2020, 2021; Nikolaidis et al., 2021; Xiong et al., 2021b; Zhao et al., 2021; Wei et al., 2022). Reliable viscosity models are required in the petroleum engineering discipline.

Friction theory (FT) combined with EoS was used for viscosity prediction (Quiñones-Cisneros et al., 2001), and viscosity was calculated by using the repulsive pressure and attractive pressure of cubic EoS. The FT model requires only a parameter that is characteristic critical viscosity. Moreover, the FT model uses cubic EoS or PC-SAFT EoS (Quiñones-Cisneros et al., 2006) as a basis to accurately model the viscosities of pure hydrocarbons and mixtures. Zéberg-Mikkelsen et al. (2002) introduced a procedure for predicting the viscosity of hydrocarbon mixtures rich in one component, and the mixture friction coefficients were estimated with mixing rules based on the values of pure component friction coefficients. Quiñones-Cisneros et al. (2004) extended the FT approach to achieve accurate *PvT* results for EoS-characterized fluid. Schmidt (2008) and Quiñones-Cisneros et al. (2012) investigated the viscosity of H_2S using the FT approach, and the calculations of FT model were consistent with experimental data. In recent

* Corresponding author.
** Corresponding author.
E-mail addresses: 18328068580@163.com (W. Xiong), 373104686@qq.com (Y.-L. Zhao).

https://doi.org/10.1016/j.petsci.2023.03.013

Nomenclature

Abbreviations

AARD	average absolute relative deviations
BIP	binary interaction parameters
CS	corresponding states
EF	expanded fluid
EoS	equation of state
ES	entropy scaling
FT	Friction theory
FV	free volume
HTHP	High-Temperature, High-Pressure
LBC	Lohrenz-Bray-Clark
MIX1	mixing rule 1
MIX2	mixing rule 2
MIX3	mixing rule 3
MIX4	mixing rule 4
MW	molecular weight, $g \cdot mol^{-1}$
NG	natural gas
PC-SAFT	Perturbed-Chain Statistical Associating Fluid Theory
PR	Peng-Robinson
PRFT	Peng-Robinson friction theory
SARA	Saturates-Aromatics-Resins-Asphaltenes
tPR	translated Peng-Robinson equation of state

Subscripts/superscripts

cal	calculated data
dis	dispersion
exp	experimental data
hc	hard-chain
hs	hard-sphere
i	component "i"
j	component "j"
mix	mixture
res	residual

Latin letters

A	molar Helmholtz free energy, J/mol
A_{ES}	the adjustable viscosity parameter of pure substance
B	the adjustable parameter of FV
B_{ES}	he adjustable viscosity parameters of pure substance
C	Péneloux-type volume translation parameters
C_{ES}	the adjustable viscosity parameters of pure substance
D_{ES}	the adjustable viscosity parameters of pure substance
F_c	correction factor of dilute gas viscosity
L	the adjustable parameter of FV
N_A	Avogadro's constant, $6.02214076 \times 10^{23}$
P	pressure, bar
P_a	PR EoS attractive pressure, bar
P_c	critical pressure, bar
P_r	PR EoS repulsive pressure, bar
R	universal gas constant, 83.145 bar $cm^3 \cdot mol^{-1}$ K^{-1}
T	temperature, K
T_c	critical temperature, K
Y	the parameters of FV or ES
Z	deviation factor
a	energy parameter, bar·cm^6/mol^2
a^{res}	residual Helmholtz free energy, J/mol
a_{ki}	the universal model constants of PC-SAFT
b	co-volume, cm^3/mol
b_{ki}	universal model constants of PC-SAFT
d	hard segment diameter, Å
g	radial distribution function
k	binary interaction parameters
k_B	Boltzmann constant, 1.380649×10^{-23} J/K
m	the number of segments
$\overline{m}$	mean segment number
s	molar residual entropy
s^*	reduced residual entropy
x	molar fraction
v	volume, cm^3/mol
v_c	critical volume, cm^3/mol
z	weighted fraction

Greek letters

α	the adjustable parameter of FV
κ_a	linear attractive viscous friction coefficient
κ_r	linear repulsive viscous friction coefficient
κ_{rr}	quadratic repulsive viscous friction coefficient
μ	total viscosity, μP
μ_0	the viscosity of dilute gas, μP
μ_{CE}	the viscosity of a pure substance, μP
μ_f	the viscosity of friction term, μP
μ^*	reduced viscosity, μP
Ω	reduced collision integral
$\Omega^{(2,2)*}$	collision integral
ω	Pitzer's acentric factor
$\Delta\mu$	the correction term of dense state
σ	temperature-independent segment diameter, Å
ρ	density, mol/cm^3
ε	the depth of potential well

years, Abutaqiya et al. (2019) used PR friction theory based on the Chi-Square characterization method and PC-SAFT FT based on the Saturates-Aromatics-Resins-Asphaltenes characterization method to model the viscosity of reservoir fluids. The FT parameters for pseudo-components were obtained by tuning to a single value of viscosity at saturation conditions. Moreover, a new fitting approach for the PC-SAFT FT model was proposed where the number of fitting parameters for each pseudo-component was reduced from two to one. Nevertheless, the use of PC-SAFT to calculate repulsive and attractive pressures in the FT model does not significantly improve the accuracy in viscosity modeling as compared to the use of PR EoS. Khemka et al. (2020) studied the viscosity modeling of crude oils under gas injection using the one-parameter friction theory framework combined with three characterization methods proposed by Khemka et al. (2021).

A free volume (FV) model based on FV concept was presented by Allal et al. (2001b), which described the variations of dynamic viscosity and density vs. pressure and temperature for dense fluid. The FV model involved only three adjustable parameters for each pure compound (Allal et al., 2001a). Moreover, it was able to represent the gas-liquid transition and the behavior in supercritical conditions. Tan et al. (2005) studied the viscosity of pure hydrocarbons by using the FT and FV models coupled with PC-SAFT EoS. De la Porte and Kossack (2014) predicted the viscosity of long-chain hydrocarbons (up to $C_{64}H_{130}$) as a function of temperatures and densities in liquid phase using FV model. The extended FV model resulted in a deviation of 5.3% for long-chain normal alkanes with carbon numbers C_6 to C_{64}. Burgess et al. (2012) used FT and FV models to model the viscosity of *n*-alkanes at temperatures up to 533 K and pressures up to 276 MPa. For *n*-alkanes, the viscosity

predictions from the modified FT model were compared with that from the FV model, but the FV model provided better viscosity modeling than the FT model for branched hydrocarbons. Moreover, accurate predictions were obtained using PC-SAFT EoS coupled with FV models. Shortly afterward, Burgess et al. (2013) extended their model using volume-translated cubic EoS and PC-SAFT density models. Llovell et al. (2013) described the viscosity of fluids using the FV model and soft-SAFT equation. The calculation results agreed with molecular simulation data, except for the deviation at density values near zero. Parvaneh et al. (2016) investigated the viscosity of nine members of the alcohol group as the polar compounds in a wide range of pressure and temperature based on a total number of 1090 viscosity set data using FV model coupled with advanced EoS. Haghbakhsh et al. (2018) modeled the viscosity of deep eutectic solvents using the FV model coupled with the association equation of state. Almasi (2015) studied the densities and viscosities of binary mixtures containing ethyl formate and 2-alkanols using FT and FV models. The FT coupled with PRSV EoS was extended to evaluate the viscosities of polar mixtures. Comparison of results of free volume theory and friction model showed that the performance of friction theory for correlating viscosities was more satisfactory because the fact that regressed parameters of this theory from experimental data were more than free volume theory and also the free volume theory had not the binary adjustable parameters for mixtures. Moreover, Almasi and Nasim (2015) studied the densities and viscosities of binary mixtures containing diethylamine and 2-propanol, 2-butanol, and 2-pentanol using the friction theory founded on the PC-SAFT model. The proposed model performed very well in all cases, with a global average absolute deviation of 3% and showed predictive capabilities for heavier compounds.

The third residual model of viscosity models for dense fluids was the expanded fluid (EF) model (Baled et al., 2018). Yarranton and Satyro (2009) presented the EF model of viscosities of pure substances by using a function based on the density of fluids, which was a form of the FV model. The EF was based on the observation that fluidity increased as the fluid expands. The EF model had two versions, including the density values from experimental data and cubic EoS (Satyro and Yarranton, 2010; Motahhari et al., 2012). Moreover, the binary interaction parameters (BIP) were required to fit experimental data.

Novak (2011a) introduced a novel entropy scaling (ES) model based on Chapman-Enskog transport coefficients to estimate the viscosity of *n*-alkanes. Moreover, the segment parameters of PC-SAFT EoS were used in the ES model to link viscosity to EoS (Novak, 2011b). Lötgering-Lin and Gross (2015) constructed a novel ES approach based on the group contribution method. A third-order polynomial was applied to calculate reduced viscosity, while the residual entropy was calculated using Polar PC-SAFT. Moreover, the ES model was extended to calculate the viscosity of mixtures (Lötgering-Lin et al., 2018). However, the model was inaccurate for the mixtures with associating components, including amines and alcohols. Fouad and Vega (2018) studied the viscosity of refrigerants using an excess ES approach. The predictions for the viscosity of refrigerants were more accurate than that from the corresponding states approach. Mairhofer (2021) presented a model for viscosity based on GERG-2008 EoS coupled with residual entropy scaling. Subsequently, Dehlouz et al. (2021) presented two models for viscosity using PR and PC-SAFT EoS, respectively. When the component-specific parameters were used, the accuracy of these models was maximal. However, the accuracy was minimal by using universal parameters. Rokni et al. (2019a, 2019b; 2021) investigated the viscosity of diesel fuels at high temperatures and high pressures (HTHP) using ES coupled with PC-SAFT. The compounds were represented as pseudo-components. However, the viscosity of mixtures containing iso-alkanes and cyclohexanes was predicted less accurately.

Recently, an alternative approach was presented to calculate viscosity, based on the Rosenfeld scaling theory, which can be applied to pure components and their mixtures in a wide range of temperatures, pressures, and compositions (Gonçalves et al., 2021). The Helmholtz scaling (A-scaling) applied the Chapman-Enskog relation, an Ansatz function, and the Polar PC-SAFT equation of state to predict viscosity. By comparing this method with the successful and consolidated entropy scaling, it was found that average absolute deviations in most pure substances and mixtures were lower for A-scaling.

Elsharkawy et al. (2003) presented a compositional model based on EoS to calculate the viscosity of crude oil. The model described temperature (T)-viscosity (μ)-pressure (P) relationships. Fan and Wang (2006) developed the viscosity model (PRμ) based on PR EoS by using the similarity between T-μ-P and P-volume (v)-T relationships. The model was accurate to calculate the viscosity of hydrocarbons. Wu et al. (2014) improved the PRμ model by replacing the universal critical compressibility factor with the real critical compressibility factor. Bonyadi and Rostami (2017) presented an EoS viscosity approach based on Soave-Redlich-Kwong EoS, which was more accurate for the viscosity of light hydrocarbons than the approach based on PR EoS.

Eighteen models based on EoS, viscosity models, and mixing rules are constructed to predict the viscosity, density, and deviation factor of natural gases at HTHP conditions. The parameters of FV and ES models are evaluated using a lot of experimental data. The volume-translated PR and PC-SAFT EoS are used to accurately calculate the densities of natural gases. Four mixing rules are used to predict the viscosities of natural gases.

2. Modeling methods

We present a review of the viscosity models used in this study, including Peng-Robinson FT (PRFT), free volume, and entropy scaling models. First, the basic equations for these models are provided for the viscosity modeling of pure substances. Then, these viscosity models are coupled with PR and PC-SAFT EoS. Finally, four mixing rules without any adjustable parameters are presented to study the viscosities of natural gases.

2.1. Peng-Robinson FT for viscosity modeling

The one-parameter PRFT model was introduced by Quiñones-Cisneros et al. (2001). In this study, the total viscosity (μ) is represented as the dilute gas term (μ_0) plus the friction term (μ_f),

$$\mu = \mu_0 + \mu_f \tag{1}$$

The dilute gas term is calculated using the approach presented by Chung et al. (1988). The approach is accurate for the viscosities of nonpolar and polar fluids over large ranges of P-v-T conditions. The dilute gas model is expressed by

$$\mu_0 = 40.785 \frac{\sqrt{MWT}}{v_c^{2/3}\Omega} F_c \tag{2}$$

where μ_0 is the viscosity of dilute gas (μP); MW is the molecular weight ($g \cdot mol^{-1}$); T is the temperature (K); v_c is the critical volume ($cm^3 \cdot mol^{-1}$); the Ω is estimated by using an empirical equation:

$$\Omega = \frac{1.16145}{T_{cm}^{0.14874}} + \frac{0.52487}{\exp(0.7732T_{cm})} + \frac{2.16178}{\exp(2.43787T_{cm})} - 6.435\times10^{-4}T_{cm}^{0.14874}\sin\left(18.0323T_{cm}^{-0.7683} - 7.27371\right) \quad (3)$$

with

$$T_{cm} = \frac{1.2593T}{T_c} \quad (4)$$

where T_c is the critical temperature (K). For non-polar gases, the F_c gives

$$F_c = 1 - 0.2756\omega \quad (5)$$

where ω is the acentric factor. And for mixtures, the μ_0 is estimated with the mixing rule as follows:

$$\mu_0 = \exp\left(\sum_i x_i \ln \mu_{0,i}\right) \quad (6)$$

where x_i is the molar fraction. The viscosity friction term μ_f in Eq. (1) is linked to the PR EoS repulsive pressure term (P_r) and PR EoS attractive pressure term (P_a) by introducing three coefficients (i.e., κ_r, κ_{rr}, and κ_a) (Quiñones-Cisneros et al., 2001):

$$\mu_f = \kappa_r P_r + \kappa_{rr} P_r^2 + \kappa_a P_a \quad (7)$$

The repulsive and attractive pressure terms in Eq. (7) are from PR EoS in section 7 of Supporting Information. The friction coefficients can be calculated by mixing rules

$$\kappa_r = \sum_i z_i \kappa_{r,i},\ \kappa_{rr} = \sum_i z_i \kappa_{rr,i},\ \kappa_a = \sum_i z_i \kappa_{a,i} \quad (8)$$

with

$$z_i = \frac{x_i}{MW_i^{0.3}\sum_j \frac{x_j}{MW_j^{0.3}}} \quad (9)$$

and $\kappa_{r,i}$, $\kappa_{rr,i}$, and $\kappa_{a,i}$ can be obtained from Quiñones-Cisneros et al. (2001). In this study, two different models (PR-PRFT and PC-SAFT-PRFT) are constructed to predict the viscosities of natural gases using the PRFT model coupled with PR and PC-SAFT, respectively (in section 7 of Supporting Information). The difference between PR-PRFT and PC-SAFT-PRFT is molar volume obtained from different EoS, and the Péneloux-type volume translation is not used for PR EoS (in section 1 of Supporting Information). The two models are used to predict the viscosities of natural gases.

2.2. FV theory

The FV model based on FV concept was presented by Allal et al. (2001a, 2001b), which described the variations of densities and viscosities vs. pressures and temperatures for dense fluids. The model divides total contributions to the viscosities of fluids into two terms, including the dense liquid term and diluted gas term (Eqs. (2)–(6))

$$\mu = \mu_0 + \Delta\mu \quad (10)$$

where $\Delta\mu$ is the correction term of dense state

$$\Delta\mu = \rho L E \sqrt{\frac{100MW}{3RT}} \exp\left(B\left(\frac{E}{RT}\right)^{3/2}\right) \quad (11)$$

with

$$E = 10^4 \alpha \rho MW + \frac{P}{\rho} \quad (12)$$

where R equates to 83.145 (bar·cm^3·mol^{-1} K^{-1}); L, α, and B are adjustable parameters, which are obtained by fitting the experimental data of pure substances. Due to the FV model requiring accurate molar density, the volume-translated PR (tPR) and PC-SAFT EoS are respectively coupled with the FV model to construct two models that are tPR-FV and PC-SAFT-FV. For mixtures, the three parameters L, α, and B are estimated using four mixing rules (in section 2 of Supporting Information)

$$Y_{mix} = \begin{cases} \text{MIX1}: \sum_i \frac{x_i Y_i}{m_i \sum_j \frac{x_j}{m_j}} \\ \text{MIX2}: \sum_i x_i Y_i \\ \text{MIX3}: \sum_i \frac{x_i Y_i}{MW_i^{0.7} \sum_j \frac{x_j}{MW_j^{0.7}}} \\ \text{MIX4}: \exp\left(\sum_i x_i \ln Y_i\right) \end{cases} \quad (13)$$

where m_i is the number of segments of ith component of PC-SAFT EoS; Y stands for L, α, and B. Using the four mixing rules, the eight models, tPR-FV-MIX1, tPR-FV-MIX2, tPR-FV-MIX3, tPR-FV-MIX4, PC-SAFT-FV-MIX1, PC-SAFT-FV-MIX2, PC-SAFT-FV-MIX3, and PC-SAFT-FV-MIX4, are constructed to predict the viscosity of natural gases. Note that no adjustable parameter is used to calculate the viscosity of mixtures in these models.

2.3. ES model for viscosity modeling

Novak (2011a) introduced a novel ES model based on Chapman-Enskog transport coefficients to calculate the viscosity of hydrocarbon. The viscosity of a pure substance is expressed as

$$\mu_{CE} = \frac{5}{16}\times10^7 \frac{\sqrt{\frac{MWk_BT}{1000mN_A\pi}}}{\sigma^2\Omega^{(2,2)*}} \quad (14)$$

where k_B is the Boltzmann constant; N_A is Avogadro's constant; σ is the segment diameter of PC-SAFT EoS (m); $\Omega^{(2,2)*}$ is the collision integral, which can be estimated using an empirical equation presented by Neufeld et al. (1972). An approximation is applied for the viscosity of mixtures

$$\mu_{CE} = \sum_i \frac{x_i \mu_{CE,i}}{\sum_j x_j \varphi_{ij}} \quad (15)$$

with

$$\varphi_{ij}=\frac{\left(1+\left(\mu_{\mathrm{CE},i}/\mu_{\mathrm{CE},j}\right)^{1/2}\left(\mathrm{MW}_j/\mathrm{MW}_i\right)^{1/4}\right)^2}{\left(8\left(1+\mathrm{MW}_i/\mathrm{MW}_j\right)\right)^{1/2}} \tag{16}$$

The reduced viscosity is expressed as

$$\mu^*=\frac{\mu}{\mu_{\mathrm{CE}}} \tag{17}$$

A third-order polynomial is used to calculate the correlation of $\ln\mu^*$ with molar residual entropy s^{res}

$$\ln\mu^*=A_{\mathrm{ES}}+B_{\mathrm{ES}}s^*+C_{\mathrm{ES}}s^{*2}+D_{\mathrm{ES}}s^{*3} \tag{18}$$

where A_{ES}, B_{ES}, C_{ES}, and D_{ES} are the adjustable viscosity parameters of pure substances; s^* is the reduced residual entropy

$$s^*=\frac{s^{\mathrm{res}}}{k_{\mathrm{B}}m} \tag{19}$$

As we all know, at a specified condition (ρ and T), the residual entropy is the derivative of residual Helmholtz free energy ($\tilde{a}^{\mathrm{res}}$) concerning T

$$\frac{s^{\mathrm{res}}(\rho,T)}{R}=-T\left[\left(\frac{\partial\tilde{a}^{\mathrm{res}}}{\partial T}\right)+\frac{\tilde{a}^{\mathrm{res}}}{T}\right] \tag{20}$$

For the different parts of molecular theory, more explanations had been published in previous literature (Gross and Sadowski, 2001). In this study, we construct two models, PR-ES and PC-SAFT-ES, based on ES coupled with PR and PC-SAFT EoS. For the PR-ES model, we did not use Péneloux-type volume translation, because we found the volume translation parameters are not necessary (in section 3 of Supporting Information). Therefore, the correlation of Péneloux-type volume translation was not used for the PR-ES model.

$$\frac{s^{\mathrm{res}}(\rho,T)}{R}=\ln\frac{v-b}{v}+\frac{\frac{\partial a(T)}{\partial T}}{2\sqrt{2}bR}\ln\frac{v+\left(\sqrt{2}+1\right)b}{v+\left(1-\sqrt{2}\right)b} \tag{21}$$

For mixtures, the four parameters A_{ES}, B_{ES}, C_{ES}, and D_{ES} are estimated using four mixing rules

$$Y_{\mathrm{mix}}=\begin{cases}\mathrm{MIX1}:\sum_i\dfrac{x_iY_i}{m_i\sum_j\frac{x_j}{m_j}}\\ \mathrm{MIX2}:\sum_i x_iY_i\\ \mathrm{MIX3}:\sum_i\dfrac{x_iY_i}{\mathrm{MW}_i^{0.7}\sum_j\frac{x_j}{\mathrm{MW}_j^{0.7}}}\\ \mathrm{MIX4}:\ln\left(\sum_i x_i\exp(Y_i)\right)\end{cases} \tag{22}$$

where Y stands for A_{ES}, B_{ES}, C_{ES}, and D_{ES}. Using the four mixing rules, the eight models, PR-ES-MIX1, PR-ES-MIX2, PR-ES-MIX3, PR-ES-MIX4, PC-SAFT-ES-MIX1, PC-SAFT-ES-MIX2, PC-SAFT-ES-MIX3, and PC-SAFT-ES-MIX4, are constructed to predict the viscosity of natural gases. Note that no adjustable parameter is used to calculate the viscosities of mixtures in these models.

3. Methodology

In this section, we introduce an approach for modeling the viscosities of natural gases as shown in Fig. 1. First, the viscosities of twenty-two pure substances in Table 1 are estimated using tPR-FV, PC-SAFT-FV, PR-ES, and PC-SAFT-ES models. Then, we test the accuracy of tPR and PC-SAFT EoS for predicting the densities of fourteen natural gas mixtures in Table 2. Accurate predictions of densities of natural gases at HTHP conditions are very important for modeling the viscosities of mixtures of natural gases using FT and FV models. Finally, sixteen models, i.e., tPR-FV-MIX1, tPR-FV-MIX2, tPR-FV-MIX3, tPR-FV-MIX4, PC-SAFT-FV-MIX1, PC-SAFT-FV-MIX2, PC-SAFT-FV-MIX3, PC-SAFT-FV-MIX4, PR-ES-MIX1, PR-ES-MIX2, PR-ES-MIX3, PR-ES-MIX4, PC-SAFT-ES-MIX1, PC-SAFT-ES-MIX2, PC-SAFT-ES-MIX3, and PC-SAFT-ES-MIX4, are constructed using tPR-FV, PC-SAFT-FV, PR-ES, and PC-SAFT-ES models coupled with four different mixing rules to predict the viscosities of seventeen natural gas mixtures. Moreover, PR-PRFT and PC-SAFT-PRFT models are used to compare with the sixteen models.

4. Results and discussion

4.1. Viscosities of pure substances

In this study, we empirically evaluate the parameters (Table 3 and Table 4) of tPR-FV, PC-SAFT-FV, PR-ES, and PC-SAFT-ES models for modeling the viscosities of pure substances. Three parameters, i.e., L, α, and B, are found to scale with MW, which indicates that the ordered behavior of parameters of PR and PC-SAFT EoS propagates to the behavior of parameter of viscosity model. Hence, the two models can be used to predict the viscosities of hydrocarbons.

Parameters, i.e., A_{ES}, B_{ES}, C_{ES}, and D_{ES}, of PR-ES and PC-SAFT-ES models are listed in Table 4. These parameters are also related to molecular weight. Moreover, the parameters of pure substances are determined by the relationships between residual entropy and reduced viscosity. The reduced viscosity vs. residual entropy is

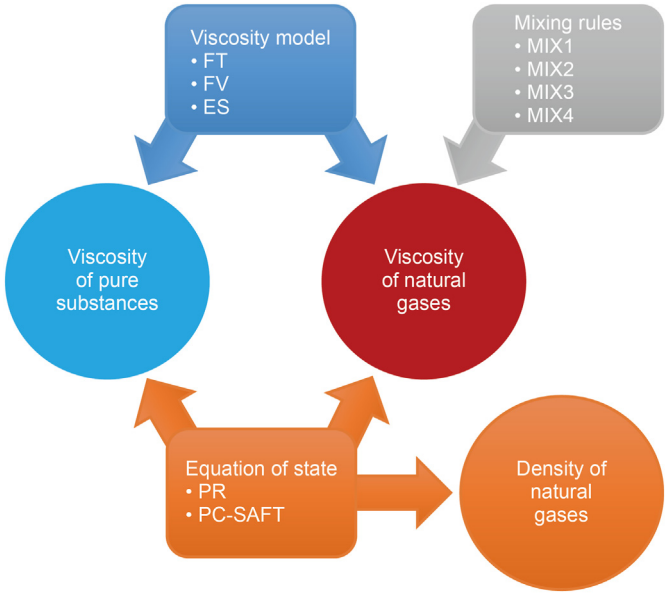

Fig. 1. A representation of the different models and methods employed in this study for modeling the viscosity of natural gases. All three elements (equation of state, viscosity model, and mixing rules) are necessary for predicting viscosity. Eighteen methodologies can be created as a result of different combinations.

Table 1
Summary of viscosity data collected from the literature.

Fluid	System	Number of data points	Impurity			Reference
			H_2S	CO_2	N_2	
Carbon dioxide	CO_2	497		✓		Stephan (1979)
Nitrogen	N_2	1146			✓	Stephan (1979)
Hydrogen sulfide	H_2S	22	✓			Quiñones-Cisneros (2012)
Methane	CH_4	584				Zéberg-Mikkelsen (2001), Quiñones-Cisneros et al. (2001)
Ethane	C_2H_6	343				Zéberg-Mikkelsen (2001), Quiñones-Cisneros et al. (2001)
Propane	C_3H_8	284				Zéberg-Mikkelsen (2001), Quiñones-Cisneros et al. (2001)
Isobutane	i-C_4H_{10}	658				Stephan (1979)
Butane	n-C_4H_{10}	243				Zéberg-Mikkelsen (2001), Quiñones-Cisneros et al. (2001)
Isopentane	i-C_5H_{12}	476				Stephan (1979)
Pentane	n-C_5H_{12}	234				Zéberg-Mikkelsen (2001), Quiñones-Cisneros et al. (2001)
Hexane	C_6H_{14}	245				Zéberg-Mikkelsen (2001), Quiñones-Cisneros et al. (2001)
Heptane	C_7H_{16}	213				Zéberg-Mikkelsen (2001), Quiñones-Cisneros et al. (2001)
Octane	C_8H_{18}	224				Zéberg-Mikkelsen (2001), Quiñones-Cisneros et al. (2001)
Nonane	C_9H_{20}	281				Stephan (1979)
Decane	$C_{10}H_{22}$	266				Zéberg-Mikkelsen (2001), Quiñones-Cisneros et al. (2001)
Undecane	$C_{11}H_{24}$	206				Stephan (1979)
Dodecane	$C_{12}H_{26}$	168				Zéberg-Mikkelsen (2001), Quiñones-Cisneros et al. (2001)
Tridecane	$C_{13}H_{28}$	168				Zéberg-Mikkelsen (2001), Quiñones-Cisneros et al. (2001)
Tetradecane	$C_{14}H_{30}$	206				Zéberg-Mikkelsen (2001), Quiñones-Cisneros et al. (2001)
Pentadecane	$C_{15}H_{32}$	258				Zéberg-Mikkelsen (2001), Quiñones-Cisneros et al. (2001)
Cetane	$C_{16}H_{34}$	207				Zéberg-Mikkelsen (2001), Quiñones-Cisneros et al. (2001)
Octadecane	$C_{18}H_{38}$	217				Zéberg-Mikkelsen (2001), Quiñones-Cisneros et al. (2001)
NG1	C_1-C_2	326				Diller (1984)
NG2	C_1-C_3	282				Giddings et al. (1966)
NG3	C_1-n-C_4	132				Carmichael et al. (1967)
NG4	C_1-CO_2	287		✓		Locke et al. (2015), Davani et al. (2013)
NG5	C_1-N_2	658			✓	Diller (1982), Davani et al. (2013)
NG6	C_2-CO_2	206		✓		Diller et al. (1988)
NG7	C_6-C_7	53				Assael et al. (1992)
NG8	C_7-C_9	57				Assael et al. (1992)
NG9	C_1-C_3-C_7	98				Al Ghafri et al. (2021)
NG10	C_1-C_3-CO_2	75		✓		Al Ghafri et al. (2018)
NG11	C_1-C_3-CO_2-N_2	129		✓	✓	Al Ghafri et al. (2019)
NG12	C_1-C_2-C_3-CO_2-N_2	32		✓	✓	Assael et al. (2001)
NG13	C_1-C_2-C_3-n-C_4-i-C_4-CO_2	47		✓		Nazeri et al. (2018)
NG14	C_1-C_2-C_3-n-C_4-i-C_4-n-C_5-i-C_5-CO_2-N_2	28		✓	✓	Kashefi et al. (2013)
NG15	C_1-C_2-C_3-n-C_4-i-C_4-n-C_5-i-C_5-CO_2-N_2-H_2S	64	✓	✓	✓	Jarrahian et al. (2015)
NG16	C_1-C_2-C_3-n-C_4-i-C_4-n-C_5-C_6-C_7-CO_2	30		✓		Lee et al. (1966)
NG17	C_1-C_2-C_3-n-C_4-i-C_4-n-C_5-C_6-C_7-CO_2-N_2	27		✓	✓	Lee et al. (1966)
Overall		9677	2	11	7	

NG represents the mixture of natural gas.

Table 2
Summary of density data collected from the literature.

System	Number of data points	AARD, %		Reference
		PR	PC-SAFT	
C_1-C_2	326	1.81	0.74	Diller (1984)
C_1-C_{10}	366	2.03	1.10	Canet et al. (2002), Regueira et al. (2016)
C_1-N_2	451	1.86	1.79	Diller (1982), Gomez-Osorio et al. (2016)
C_1-CO_2	119	1.79	1.14	Locke et al. (2015)
C_2-CO_2	206	1.90	0.78	Diller et al. (1988)
C_3-C_{10}	233	1.80	1.25	Bamgbade et al. (2015)
C_6-C_7	53	1.06	0.44	Assael et al. (1992)
C_7-C_9	57	0.39	0.44	Assael et al. (1992)
C_1-C_3-C_7	98	1.96	1.66	Al Ghafri et al. (2021)
C_1-C_3-CO_2	75	1.70	1.02	Al Ghafri et al. (2018)
C_1-C_3-CO_2-N_2	129	0.88	0.90	Al Ghafri et al. (2019)
C_1-C_2-C_3-CO_2-N_2	32	0.83	1.08	Assael et al. (2001)
C_1-C_2-C_3-i-C_4-n-C_4-C_5-C_6-C_7-CO_2	62	5.39	3.47	Lee et al. (1966)
C_1-C_2-C_3-i-C_4-n-C_4-C_5-C_6-C_7-CO_2-N_2	38	2.75	0.62	Lee et al. (1966)
Overall AARD, %	2245	1.86	1.21	

shown in Fig. S7 for pure substances. Fig. S7a, c, and e are calculated from PC-SAFT EoS, while other figures are from PR EoS. At first glance, the ranges of residual entropy of PC-SAFT EoS are less than that of PR EoS. Moreover, the degree of linearity between residual entropy and reduced viscosity from PC-SAFT model exceeds that of PR model. In Fig. S7a–d, the PR and PC-SAFT are accurate to describe the relationships between reduced viscosity and residual entropy using a third-order polynomial. However, the PR EoS is not suitable for modeling the viscosity of heavy hydrocarbons as shown in Fig. S7f. For PC-SAFT EoS, because predictions of volume are

Table 3
The parameters of tPR-FV and PC-SAFT-FV models for modeling the viscosity of pure substances.

Substance	tPR-FV			PC-SAFT-FV			AARD, %	
	L	α	B	L	α	B	tPR-FV	PC-SAFT-FV
CO_2	0.4700	33.6	0.0020	0.6000	21.2	0.0126	1.06	0.79
N_2	0.6700	11.2	0.0150	0.7600	7.9	0.0290	2.88	3.06
H_2S	0.9900	27.6	0.0001	1.1600	21.1	0.0033	2.77	2.98
CH_4	1.0636	21.3	0.0162	1.0300	22.6	0.0149	2.91	3.56
C_2H_6	1.0145	34.9	0.0132	0.9893	35.6	0.0119	2.61	2.74
C_3H_8	0.9653	48.8	0.0114	0.9486	49.6	0.0101	2.52	3.40
i-C_4H_{10}	0.9163	63.5	0.0101	0.9080	65.9	0.0088	3.94	3.23
n-C_4H_{10}	0.9163	61.3	0.0101	0.9080	63.2	0.0088	2.45	2.82
i-C_5H_{12}	0.8672	71.9	0.0091	0.8673	77.5	0.0078	7.75	5.75
n-C_5H_{12}	0.8672	72.7	0.0091	0.8673	77.8	0.0078	3.74	1.95
C_6H_{14}	0.8181	88.7	0.0083	0.8266	91.8	0.0070	4.85	3.07
C_7H_{16}	0.7690	100.7	0.0075	0.7859	108.2	0.0062	2.84	1.66
C_8H_{18}	0.7199	118.0	0.0069	0.7452	126.0	0.0056	2.74	2.55
C_9H_{20}	0.6708	132.6	0.0064	0.7045	146.4	0.0051	1.24	1.22
$C_{10}H_{22}$	0.6217	152.1	0.0059	0.6639	168.2	0.0046	2.26	1.29
$C_{11}H_{24}$	0.5726	168.2	0.0055	0.6232	191.1	0.0042	1.32	1.47
$C_{12}H_{26}$	0.5236	189.8	0.0051	0.5826	217.1	0.0038	2.34	1.94
$C_{13}H_{28}$	0.4743	205.4	0.0047	0.5417	246.2	0.0034	1.30	1.58
$C_{14}H_{30}$	0.4253	223.7	0.0043	0.5011	271.8	0.0030	2.92	3.11
$C_{15}H_{32}$	0.3763	249.2	0.0040	0.4605	309.6	0.0027	1.87	1.36
$C_{16}H_{34}$	0.3273	275.6	0.0037	0.4199	348.2	0.0024	2.06	1.98
$C_{18}H_{38}$	0.2289	365.8	0.0032	0.3385	443.7	0.0019	4.46	4.36
Overall AARD, %							3.03	2.74

Table 4
The parameters of PR-ES and PC-SAFT-ES models for modeling the viscosity of pure substances.

Substance	PR-ES				PC-SAFT-ES				AARD, %	
	D_{ES}	C_{ES}	B_{ES}	A_{ES}	D_{ES}	C_{ES}	B_{ES}	A_{ES}	PR-ES	PC-SAFT-ES
CO_2	−0.052812	−0.021	−1.552	−0.442	−0.043276	0.094	−1.523	−0.438	6.10	3.83
N_2	−0.033600	−0.142	−1.304	−0.181	−0.030895	−0.085	−1.178	−0.204	4.42	5.45
H_2S	−0.040896	−0.264	−1.750	−0.366	−0.035937	−0.256	−1.723	−0.356	4.40	4.07
CH_4	−0.019248	−0.150	−1.120	−0.115	−0.019474	−0.072	−1.013	−0.097	3.54	3.32
C_2H_6	−0.036084	−0.278	−1.815	−0.398	−0.032663	−0.221	−1.700	−0.368	2.51	2.39
C_3H_8	−0.052920	−0.384	−2.192	−0.561	−0.043338	−0.287	−2.036	−0.511	2.33	1.97
i-C_4H_{10}	−0.069744	−0.375	−2.345	−0.610	−0.052150	−0.321	−2.293	−0.600	6.59	4.90
n-C_4H_{10}	−0.069744	−0.469	−2.432	−0.667	−0.052150	−0.347	−2.288	−0.644	2.79	1.60
i-C_5H_{12}	−0.086580	−0.501	−2.381	−0.479	−0.059558	−0.350	−2.242	−0.450	4.15	3.33
n-C_5H_{12}	−0.086580	−0.557	−2.569	−0.645	−0.059558	−0.384	−2.391	−0.597	4.26	1.41
C_6H_{14}	−0.103416	−0.610	−2.678	−0.648	−0.065867	−0.387	−2.456	−0.581	4.36	1.59
C_7H_{16}	−0.120252	−0.674	−2.838	−0.727	−0.071306	−0.433	−2.720	−0.750	4.93	1.06
C_8H_{18}	−0.137076	−0.768	−3.069	−0.828	−0.076040	−0.475	−2.959	−0.907	5.87	2.06
C_9H_{20}	−0.153912	−0.677	−2.562	−0.205	−0.080202	−0.400	−2.734	−0.600	4.30	0.93
$C_{10}H_{22}$	−0.170748	−0.815	−3.019	−0.596	−0.083889	−0.286	−2.480	−0.350	7.07	0.70
$C_{11}H_{24}$	−0.187560	−0.946	−3.239	−0.671	−0.087173	−0.353	−2.784	−0.611	5.94	0.86
$C_{12}H_{26}$	−0.204360	−1.004	−3.469	−0.868	−0.090118	−0.284	−2.626	−0.421	9.18	1.31
$C_{13}H_{28}$	−0.221280	−1.161	−3.813	−1.098	−0.092794	−0.330	−2.800	−0.435	10.22	1.15
$C_{14}H_{30}$	−0.238080	−1.384	−4.342	−1.499	−0.095204	−0.162	−2.266	−0.001	8.52	3.13
$C_{15}H_{32}$	−0.254880	−1.469	−4.662	−1.800	−0.097400	−0.249	−2.669	−0.313	10.02	2.01
$C_{16}H_{34}$	−0.271680	−1.622	−5.045	−2.000	−0.099409	−0.171	−2.473	−0.114	9.43	2.63
$C_{18}H_{38}$	−0.305400	−1.783	−5.450	−2.298	−0.102968	−0.002	−2.048	0.278	9.55	2.85
Overall AARD, %									5.48	3.01

accurate, the correlations between reduced viscosity and residual entropy are very well as shown in Fig. S7e. Moreover, because PR EoS cannot accurately calculate the molar volume of heavy hydrocarbons at high pressures, the calculated reduced viscosity is larger than its actual value. We plotted reduced viscosity vs. molar volume diagram as shown in Fig. S6. The results show that PR EoS cannot correctly calculate the molar volume change with pressure, but the PC-SAFT EoS can correctly describe the behavior.

We calculated the viscosities of pure substances in Fig. S8 using tPR-FV, PC-SAFT-FV, PR-ES, and PC-SAFT-ES models. Fig. S8a–d show that the four models are suitable for modeling the viscosities of light hydrocarbons, CO_2, N_2, and H_2S. Moreover, for heavy hydrocarbons in Fig. S8e–h, some deviations are found at the viscosity values above 50,000 μP, low temperatures, and high pressures. It is worth noting that Fig. S8g indicates that the calculations of PR-ES model are inaccurate for the viscosity of heavy hydrocarbons (the errors increase with increasing the number of carbon atoms) because PR EoS cannot accurately calculate the molar volume of heavy hydrocarbons at high pressures. Average absolute relative deviations (AARD, Eq. (23)) of tPR-FV, PC-SAFT-FV, PR-ES, and PC-SAFT-ES models for the viscosities of pure substances are 3.03%, 2.74%, 5.48%, and 3.01%, respectively. The performance of PR-ES model is poor for heavy hydrocarbons in Tables 3 and 4 and Fig. S9, especially $C_{12}H_{26}$ to $C_{18}H_{38}$, because PR EoS cannot correctly calculate the molar volume at high pressures.

$$\mathrm{AARD} = \frac{1}{n}\sum_{i=1}^{n}\frac{\left|\mu_i^{\mathrm{exp}} - \mu_i^{\mathrm{cal}}\right|}{\mu_i^{\mathrm{exp}}} \tag{23}$$

where μ^{exp} is experimental data in μP; μ^{cal} is calculated data in μP.

Quiñones-Cisneros et al. (2001) evaluated the viscosities of pure components using the FT model. For PRFT model, they proposed three reduced critical isotherm friction parameters and thirteen residual friction parameters. In this study, we used these parameters to model the viscosity of mixtures, because the PRFT model produced a satisfactory performance for the viscosity of pure *n*-alkanes (AARD = 2.02%) (Quiñones-Cisneros et al., 2001). This may be due to the fact that regressed parameters of this theory from experimental data are more than FV theory and ES model (for each substance, the corresponding linear *f*-theory model consists of seven adjustable parameters). More details about modeling the viscosities of pure components can be found in the study of Quiñones-Cisneros et al. (2001).

4.2. Densities of natural gases

Correct calculation of densities of natural gases is vital to accurately model the viscosities of natural gases. In this study, we evaluated the performance of tPR and PC-SAFT EoS for predicting the densities and deviation factors (*Z*-Factor) of natural gases.

We test the densities of natural gases from a lot of literature in Table 2 using tPR and PC-SAFT EoS. Fig. S10 shows that the predictions of PC-SAFT EoS for densities of mixtures in gas, liquid, and supercritical conditions are more accurate than that of the volume-translated PR EoS. Moreover, the AARD of prediction of tPR and PC-SAFT EoS in Table 2 for densities of fourteen mixtures are 1.86% and 1.21%, respectively. Fig. S11 shows that PC-SAFT EoS is more accurate for predicting the densities of natural gases than tPR model. This may be attributed to the flexible attractive and repulsive terms of PC-SAFT equation of state used for calculating molar volume.

We test the deviation factors of two sample gases (Liu et al., 2019) listed in Table S8 at high-temperature and ultra-high-pressure conditions. As shown in Fig. S12, tPR and PC-SAFT EoS can accurately predict the *Z*-Factor values of two sample gases. However, to our surprise, the predictions of tPR EoS for *Z*-Factor are more accurate than that of PC-SAFT EoS. As we all know, the PC-SAFT EoS is better for predicting volume than volume-translated PR EoS. This may be attributed to different BIPs used for calculating the deviation factors.

4.3. Viscosities of natural gases

Eighteen models, PR-PRFT, PC-SAFT-PRFT, tPR-FV-MIX1, tPR-FV-MIX2, tPR-FV-MIX3, tPR-FV-MIX4, PC-SAFT-FV-MIX1, PC-SAFT-FV-MIX2, PC-SAFT-FV-MIX3, PC-SAFT-FV-MIX4, PR-ES-MIX1, PR-ES-MIX2, PR-ES-MIX3, PR-ES-MIX4, PC-SAFT-ES-MIX1, PC-SAFT-ES-MIX2, PC-SAFT-ES-MIX3, and PC-SAFT-ES-MIX4, are constructed to predict the viscosities of natural gases by combining different EoS, viscosity models, and mixing rules. Note that no adjustable parameter is used to calculate the viscosities of natural gases in these models. Compositions of natural gas, i.e., NG1 to NG17, are listed in Tables S3 and S4.

Predictions of these models for seventeen mixtures of natural gases are shown in Fig. S13. At first glance, the PC-SAFT-PRFT model produces the largest deviation, because the PRFT viscosity model requires molar volume obtained by classical PR EoS without volume translation. Predictions of tPR-FV-MIX4, PC-SAFT-FV-MIX4, and PC-SAFT-ES-MIX2 models agree with experimental data. Overall, the accuracy of FV family models is better than that of ES family models, and ES family models are superior to PRFT family models. On the other hand, PC-SAFT family models for calculating viscosity are usually more accurate than PR family models, because predictions of PC-SAFT for molar volume are more accurate.

Fig. 2 plots the predictions of PC-SAFT-PRFT, PC-SAFT-FV-MIX4, and PC-SAFT-ES-MIX4 models for natural gases of NG13, NG14, and NG15 compared with experimental data at HTHP conditions. Fig. 2a shows that the three models accurately predict the viscosities of NG13 at low pressures. However, predictions of PC-SAFT-FV-MIX4 and PC-SAFT-ES-MIX4 models are larger than experimental data at high pressures, while predictions of PC-SAFT-PRFT model match experimental data. Fig. 2b and c indicate that the accuracy of PC-SAFT-ES-MIX4 is superior to that of PC-SAFT-FV-MIX4 at the pressure of up to 1400 bar and the temperature of up to 473.15 K, while PC-SAFT-FV-MIX4 is better than PC-SAFT-PRFT. CO_2 content in NG13 is 69.99%, while CH_4 content in NG14 and NG15 is above 71%. The accuracy of predictions of PC-SAFT-PRFT decreases with increasing CH_4 content, which indicates that the model is suitable for mixtures with high CO_2 content. Moreover, PC-SAFT-FV-MIX4 and PC-SAFT-ES-MIX4 models are suitable for mixtures with high CH_4 content.

AARD of eighteen models for the viscosities of natural gases at all conditions is shown in Table S9 and Fig. S14. MIX4 is the most suitable for FV family models followed by MIX2, MIX1, and MIX3. For ES family models, MIX2 produces the best accuracy followed by MIX3, MIX1, and MIX4. Moreover, AARD of the best accurate three models, i.e., PC-SAFT-FV-MIX4, tPR-FV-MIX4, and PC-SAFT-ES-MIX2, are 5.66%, 6.27%, and 6.50%, respectively. Note that it is difficult to accurately predict the viscosity of each natural gas using a single model. As shown in Fig. S14b, the AARD of PC-SAFT-FV-MIX4 for NG1 is not minimum, although the model produces better accuracy for the other natural gases.

4.4. Comparison to the existing industrial models for viscosity

In this study, we used two existing industrial models, i.e., corresponding states (CS) theory (Pedersen et al., 1984, 1987; Lindeloff et al., 2003) and LBC (Lohrenz et al., 1964), coupled with translated PR and PC-SAFT EoS (in sections 5 and 6 of Supporting Information), and we constructed four models that are tPR-CS, PC-SAFT-CS, tPR-LBC, and PC-SAFT-LBC. Unfortunately, the predicted viscosities of these models are far from experimental data as shown in Fig. S15 and the results cannot satisfy industrial accuracy. However, these models are usually used for modeling the viscosity of oil with petroleum fractions and plus fractions. In our view, it is very difficult to accurately model the viscosity of more complex mixtures using a model which is inaccurate for modeling the viscosity of simple mixtures (such as NG1 to NG17). There is a commonly used approach that is adjusting the parameters of petroleum fractions and plus fractions to fit the experimental data of viscosity.

As shown in Table S10 and Fig. S16, the CS model is inaccurate for predicting the viscosities of binary and ternary mixtures but it can be used to calculate the viscosities of multicomponent mixtures. The main factor affecting the performance is not the number of components but methane concentration, because the CS model takes methane as a reference fluid. Conversely, the LBC model is more accurate for the viscosities of binary and ternary mixtures than that of multicomponent mixtures. Overall, the performance of LBC model is better than that of CS model. Moreover, these models are inaccurate compared with the proposed FV and ES models.

The characterization methods are promising to model the viscosity of reservoir fluids. To use PR EoS for modeling phase behavior, three parameters are required for each component: critical temperature (T_c), critical pressure (P_c), and acentric factor (ω). In this work, we present some empirical correlations to estimate

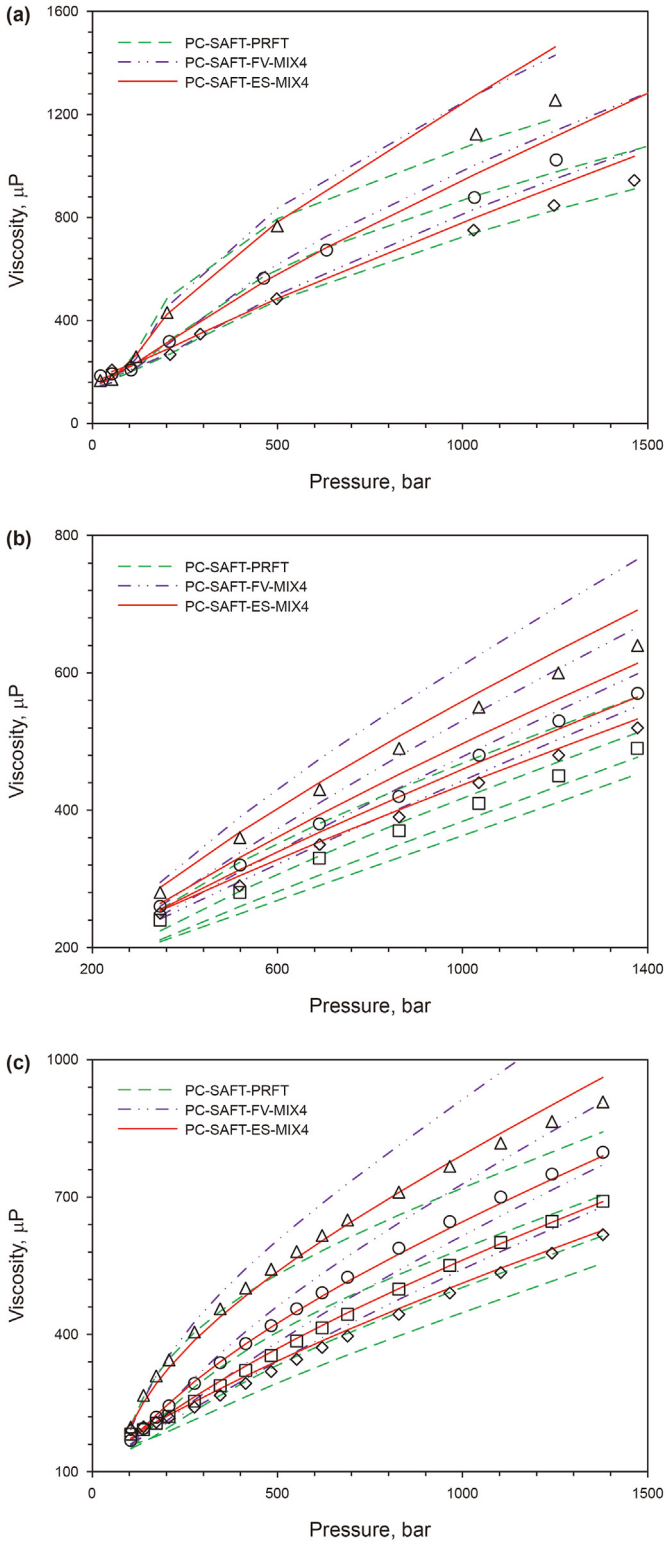

Fig. 2. Predicted viscosity vs. pressure diagrams for natural gases. (**a**): NG13; (**b**): NG14; (**c**): NG15. (**a**) triangle: 323.2 K; circle: 373.2 K; rhombus: 423.2 K; (**b**) triangle: 323.15 K; circle: 373.15 K; rhombus: 423.15 K; square: 473.15 K; (**c**) triangle: 277.78 K; circle: 333.33 K; square: 388.89 K; rhombus: 444.44 K. Experimental data taken from Nazeri et al. (2018), Kashefi et al. (2013), and Jarrahian et al. (2015).

the parameters of pseudo-components for PR EoS

$$T_c = -0.0093938MW^2 + 4.53911MW + 1.720296 \quad (24)$$

$$P_c = 7.2992 \times 10^{-4}MW^2 - 0.350636MW + 55.990326 \quad (25)$$

$$\omega = 0.0033MW + 0.011 \quad (26)$$

$$v_c = 4.0033MW + 27.5074 \quad (27)$$

and the following correlations were used for PC-SAFT EoS (Khemka et al., 2021)

$$m = 0.0257MW + 0.8444 \quad (28)$$

$$\sigma = -4.8013\frac{\ln(MW)}{MW} + 4.047 \quad (29)$$

$$\frac{\varepsilon}{k_B} = \exp\left(5.5769 - \frac{9.523}{MW}\right) \quad (30)$$

Three parameters, i.e., L, α, and B, for tPR-FV are found to scale with MW, which can be estimated using the following correlations

$$L = -0.0035MW + 1.1197 \quad (31)$$

$$\alpha = 0.0033758MW^2 + 0.395279MW + 24.10322 \quad (32)$$

$$B = 2.3841 \times 10^{-7}MW^2 - 1.0883 \times 10^{-4}MW + 0.01622 \quad (33)$$

and the following correlations were used for PC-SAFT-FV

$$L = -0.0029MW + 1.0765 \quad (34)$$

$$\alpha = 0.0052648MW^2 + 0.233519MW + 28.479582 \quad (35)$$

$$B = 2.3841 \times 10^{-7}MW^2 - 1.0883 \times 10^{-4}MW + 0.01492 \quad (36)$$

For PC-SAFT-ES, we used the following correlations

$$D_{ES} = \frac{1}{-6.911 - \frac{712.8}{MW}} \quad (37)$$

$$C_{ES} = 2.0037 \times 10^{-5}MW^2 - 0.0045657MW - 0.134382 \quad (38)$$

$$B_{ES} = 6.5087 \times 10^{-5}MW^2 - 0.019499MW - 1.298312 \quad (39)$$

$$A_{ES} = 4.0178 \times 10^{-5}MW^2 - 0.0083234MW - 0.212967 \quad (40)$$

In this study, we predicted the viscosity of gas condensate (GCB00-1) measured by Kashefi et al. (2013). GCB00-1 was gravimetrically prepared by 'livening' a fully characterized dead condensate with a natural gas (composition given in Table S11). The characterization of the dead condensate included its fractionation into single carbon number cuts from C_{6s} through to C_{25s}, on each of which molecular weight and density measurements were made, as well as for the C_{26+} distillation residue (Table S11). The predictions of Pedersen (Kashefi et al., 2013), LBC (Kashefi et al., 2013), HW2

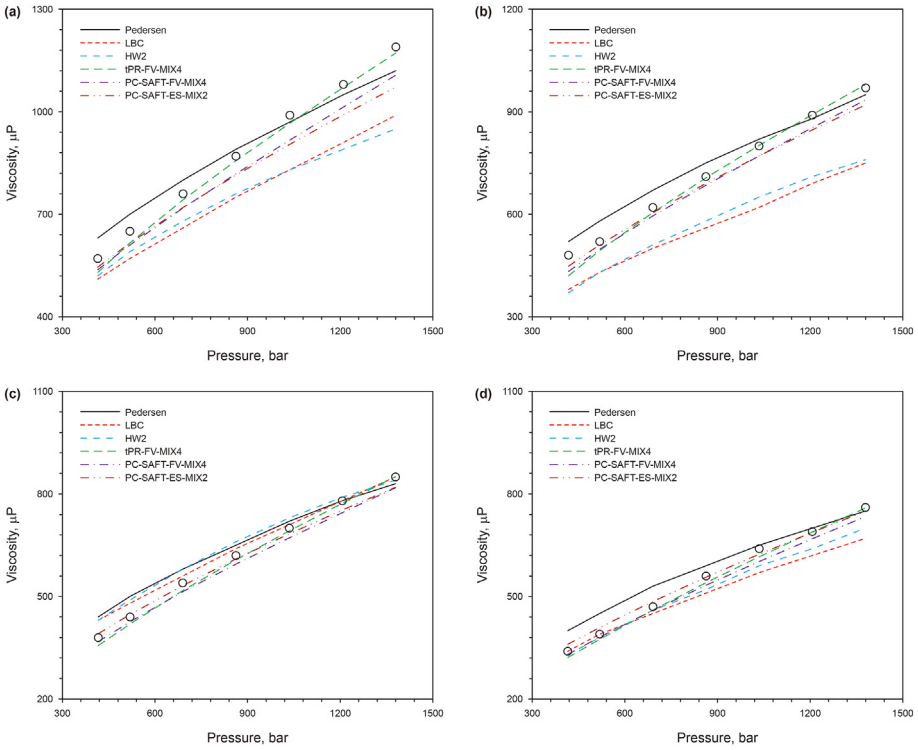

Fig. 3. Predicted viscosity vs. pressure diagrams for GCB00-1. (**a**) 323.15 K; (**b**) 373.15 K; (**c**) 423.15 K; (**d**) 473.15 K. Experimental data taken from Kashefi et al. (2013).

Table 5
Measured and predicted viscosities of the gas condensate (GCB00-1).

T, K	*P*, bar	*μ*, μP	Pedersen	LBC	HW2	tPR-FV-MIX4	PC-SAFT-FV-MIX4	PC-SAFT-ES-MIX2
323.15	414.5	570	630	510	520	529.45	537.50	545.13
323.15	518.8	650	700	570	590	615.44	609.73	615.58
323.15	690.9	760	800	660	680	741.88	717.88	719.75
323.15	862.3	870	890	750	760	856.38	818.35	814.35
323.15	1036.8	990	970	830	830	966.13	916.98	904.81
323.15	1210.7	1080	1050	910	890	1071.44	1013.58	991.01
323.15	1380.6	1190	1120	990	950	1172.10	1107.49	1072.58
373.15	417.2	480	520	380	370	419.89	432.62	447.70
373.15	518.8	520	580	430	430	493.05	497.08	509.87
373.15	690.2	620	670	500	510	604.46	594.84	604.23
373.15	862.3	710	750	560	580	706.06	684.88	690.24
373.15	1034.6	800	820	620	650	801.09	770.42	770.53
373.15	1207.1	890	880	690	710	891.84	853.42	846.80
373.15	1379.7	970	950	750	760	979.73	935.02	920.08
423.15	416.1	380	440	430	430	356.49	368.06	391.35
423.15	519.0	440	500	480	490	419.50	425.86	446.87
423.15	690.0	540	580	560	580	516.76	513.48	531.43
423.15	862.1	620	650	640	660	607.00	594.63	609.61
423.15	1035.0	700	720	710	730	691.99	671.68	683.18
423.15	1206.8	780	780	780	790	772.39	745.39	752.61
423.15	1379.5	850	830	850	840	850.31	817.69	819.57
473.15	415.2	340	400	340	330	321.52	330.61	360.18
473.15	518.6	390	450	390	380	374.94	381.14	409.39
473.15	690.7	470	530	450	460	460.13	459.55	485.61
473.15	862.9	560	590	510	520	540.36	532.66	556.67
473.15	1035.1	640	650	570	590	616.33	602.05	623.84
473.15	1207.0	690	700	620	640	688.79	668.74	687.89
473.15	1379.4	760	750	670	700	758.86	733.83	749.71
Overall AARD, %			6.36	11.48	11.24	2.91	4.62	4.00

(Kashefi et al., 2013), tPR-FV-MIX4, PC-SAFT-FV-MIX4, and PC-SAFT-ES-MIX2 models are shown in Fig. 3. The proposed models are consistent with experimental data, while the Pedersen, LBC, and HW2 models from Kashefi et al. (2013) produce larger deviations. Predictions of Pedersen's model are larger than experimental data at the pressure below 1000 bar. Pedersen's model is inaccurate for GCB00-1 because CH_4 content is 69.62%, while the other components are 30.38%. LBC and HW2 models were empirical correlations between viscosity and the fourth-degree polynomial of the reduced density. It is very difficult to predict

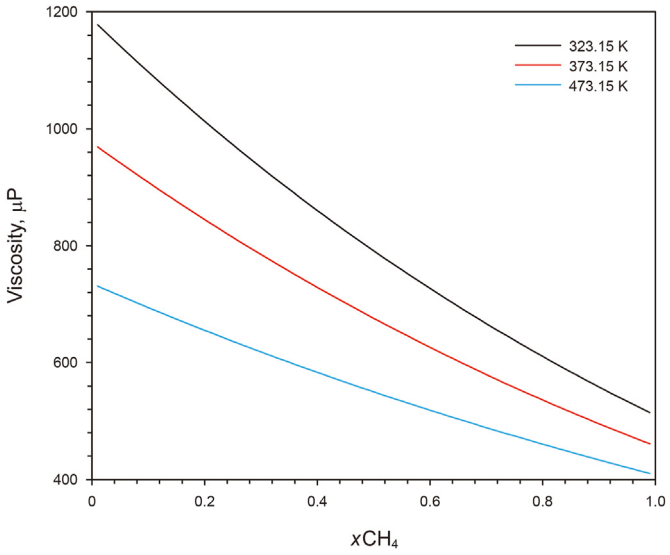

Fig. 4. Predicted viscosity vs. molar fraction for NG1. $P = 1000$ bar.

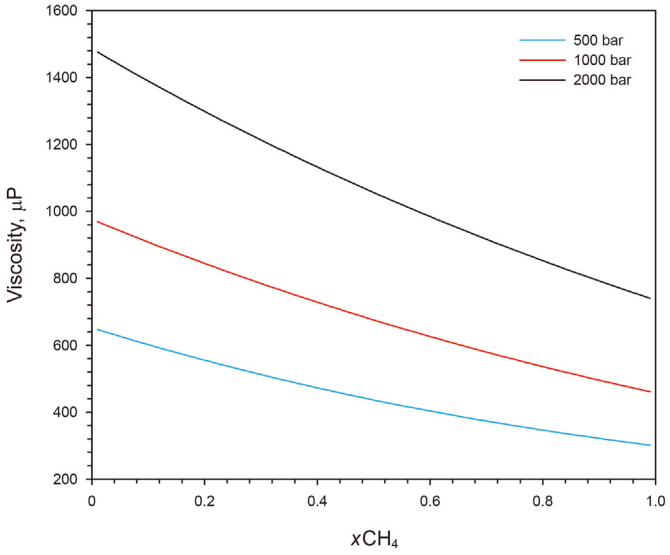

Fig. 5. Predicted viscosity vs. molar fraction for NG1. $T = 373.15$ K.

the viscosities of hydrocarbon mixtures using simple LBC and HW2 correlation in Fig. 3, especially in high temperature and pressure conditions. A great advantage is that our proposed models, especially tPR-FV-MIX4, are accurate for the viscosity of natural gas at HTHP conditions. The measured and predicted viscosities of gas condensate are given in Table 5, AARD of the best accurate three models (i.e., tPR-FV-MIX4, PC-SAFT-ES-MIX2, and PC-SAFT-FV-MIX4) are 2.91%, 4.00%, and 4.62%, respectively, which shows that the proposed models are suitable for complex natural gas.

Modeling the viscosities of reservoir fluids with petroleum fractions and plus fractions is not the focus of this study, such as the simulation of a CVD test. Instead, we analyze the effects of gas composition changes on viscosity using NG1 (C_1 to C_2) which is a simple system but has a better description. Fig. 4 shows that the viscosity of C_1-C_2 system decreases with increasing the molar fraction of methane at 1000 bar. Moreover, at the same condition, the viscosity of C_1-C_2 system decreases with increasing temperature. Fig. 5 shows that the viscosity of C_1-C_2 system increases with increasing pressure.

5. Conclusions

Eighteen models based on two equations of state, three viscosity models, and four mixing rules were constructed to predict the viscosities of natural gases at HTHP conditions. The following five major conclusions are drawn from this work.

- The parameters of FV and ES models are found to scale with MW, which indicates that the ordered behavior of parameter of PR and PC-SAFT EoS propagates to the behavior of parameter of viscosity model.
- The MIX4 is the most suitable for FV family models, while the MIX2 for ES family models produces the best accuracy.
- The FV family models are more accurate for predicting the viscosity of natural gases than ES family models at HTHP conditions, while the ES family models are superior to PRFT family models.
- The AARD of the best accurate three models, PC-SAFT-FV-MIX4, tPR-FV-MIX4, and PC-SAFT-ES-MIX2, are 5.66%, 6.27%, and 6.50%, respectively, which is available for industrial production.
- Compared with the existing industrial models (CS and LBC), the proposed three models were more accurate for modeling the viscosity of natural gas, including gas condensate.
- Using characterization methods, the proposed models are easy to be extended to predict the viscosity of complex natural gas. We accurately predicted the viscosity of gas condensate, including fifteen pseudo-components and plus fractions.

Declaration of competing interest

The authors declare that they have no known competing financial interests or personal relationships that could have appeared to influence the work reported in this paper.

Acknowledgments

This work was supported by the China Scholarship Council (No. 202209225014), National Science Fund for Excellent Young Scholars (Grant No. 52222402), National Natural Science Foundation of China (Grant No. 52234003), National Natural Science Foundation of China (Grant No. 52074235), National Science and Technology Major Project of China during the 13th Five-Year Plan Period (2016ZX05062), Sichuan Science and Technology Program (Grant No. 2021YJ0345), National Natural Science Foundation of China (Grant No. 51874251, 51774243, 52174036, and 51704247), Sichuan Science and Technology Program (NO. 2022JDJQ0009) and shale gas industry development Institute of Sichuan province, International S&T Cooperation Program of Sichuan Province (Grant No. 2019YFH0169), the Deep Marine shale gas efficient development Overseas Expertise Introduction Center for Discipline Innovation (111 Center), and Science and Technology Cooperation Project of the CNPC-SWPU Innovation Alliance (No.2020CX020202, 2020CX030202). The authors would also like to appreciate the editors and reviewers, whose critical comments were very helpful in preparing this article.

Appendix A. Supplementary data

Supplementary data related to this article can be found at https://doi.org/10.1016/j.petsci.2023.03.013.

References

Abutaqiya, M.I., Zhang, J., Vargas, F.M., 2019. Viscosity modeling of reservoir fluids using the Friction Theory with PC-SAFT crude oil characterization. Fuel 235, 113–129. https://doi.org/10.1016/j.fuel.2018.06.062.

Al Ghafri, S.Z., Czubinski, F.F., May, E.F., 2018. Viscosity measurements of (CH_4+C_3H_8+CO_2) mixtures at temperatures between (203 and 420) K and pressures between (3 and 31) MPa. Fuel 231, 187–196. https://doi.org/10.1016/j.fuel.2018.05.087.

Al Ghafri, S.Z., McKenna, A., Czubinski, F.F., et al., 2019. Viscosity of (CH_4+C_3H_8+CO_2+N_2) mixtures at temperatures between (243 and 423) K and pressures between (1 and 28) MPa: experiment and theory. Fuel 251, 447–457. https://doi.org/10.1016/j.fuel.2019.04.017.

Al Ghafri, S.Z., Akhfash, M., Hughes, T.J., et al., 2021. High pressure viscosity measurements of ternary (methane+propane+heptane) mixtures. Fuel Process. Technol. 223, 106984. https://doi.org/10.1016/j.fuproc.2021.106984.

Allal, A., Boned, C., Baylaucq, A., 2001a. Free-volume viscosity model for fluids in the dense and gaseous states. Phys. Rev. 64 (1), 011203. https://doi.org/10.1103/PhysRevE.64.011203.

Allal, A., Moha-Ouchane, M., Boned, C., 2001b. A new free volume model for dynamic viscosity and density of dense fluids versus pressure and temperature. Phys. Chem. Liq. 39 (1), 1–30. https://doi.org/10.1080/00319100108030323.

Almasi, M., 2015. Densities and viscosities of binary mixtures containing ethyl formate and 2-alkanols: friction theory and free volume theory. J. Chem. Eng. Data 60 (3), 714–720. https://doi.org/10.1021/je500848q.

Almasi, M., Nasim, H., 2015. Thermodynamic and transport properties of binary mixtures; friction theory coupled with PC-SAFT model. J. Chem. Therm. 89, 1–6. https://doi.org/10.1016/j.jct.2015.04.017.

Assael, M.J., Charitidou, E., Dymond, J.H., et al., 1992. Viscosity and thermal conductivity of binary *n*-heptane+ *n*-alkane mixtures. Int. J. Thermophys. 13 (2), 237–249. https://doi.org/10.1007/BF00504434.

Assael, M.J., Dalaouti, N.K., Vesovic, V., 2001. Viscosity of natural-gas mixtures: measurements and prediction. Int. J. Thermophys. 22 (1), 61–71. https://doi.org/10.1023/A:1006784814390.

Baled, H.O., Gamwo, I.K., Enick, R.M., et al., 2018. Viscosity models for pure hydrocarbons at extreme conditions: a review and comparative study. Fuel 218, 89–111. https://doi.org/10.1016/j.fuel.2018.01.002.

Bamgbade, B.A., Wu, Y., Burgess, W.A., et al., 2015. Measurements and modeling of high-temperature, high-pressure density for binary mixtures of propane with *n*-decane and propane with *n*-eicosane. J. Chem. Therm. 84, 108–117. https://doi.org/10.1016/j.jct.2014.12.015.

Bian, X.Q., Xiong, W., Kasthuriarachchi, D.T.K., et al., 2019. Phase equilibrium modeling for carbon dioxide solubility in aqueous sodium chloride solutions using an association equation of state. Ind. Eng. Chem. Res. 58 (24), 10570–10578. https://doi.org/10.1021/acs.iecr.9b01736.

Bonyadi, M., Rostami, M., 2017. A new viscosity model based on Soave-Redlich-Kwong equation of state. Fluid Phase Equil. 451, 40–47. https://doi.org/10.1016/j.fluid.2017.07.009.

Burgess, W.A., Tapriyal, D., Gamwo, I.K., et al., 2012. Viscosity models based on the free volume and frictional theories for systems at pressures to 276 MPa and temperatures to 533 K. Ind. Eng. Chem. Res. 51 (51), 16721–16733. https://doi.org/10.1021/ie301727k.

Burgess, W.A., Tapriyal, D., Morreale, B.D., et al., 2013. Volume-translated cubic EoS and PC-SAFT density models and a free volume-based viscosity model for hydrocarbons at extreme temperature and pressure conditions. Fluid Phase Equil. 359, 38–44. https://doi.org/10.1016/j.fluid.2013.07.016.

Canet, X., Baylaucq, A., Boned, C., 2002. High-pressure (up to 140 MPa) dynamic viscosity of the methane+decane system. Int. J. Thermophys. 23 (6), 1469–1486. https://doi.org/10.1023/A:1020781715494.

Carmichael, L.T., Berry, V.M., Sage, B.H., 1967. Viscosity of a mixture of methane and butane. J. Chem. Eng. Data 12 (1), 44–47. https://doi.org/10.1021/je60032a014.

Chung, T.H., Ajlan, M., Lee, L.L., et al., 1988. Generalized multiparameter correlation for nonpolar and polar fluid transport properties. Ind. Eng. Chem. Res. 27 (4), 671–679. https://doi.org/10.1021/ie00076a024.

Davani, E., Falcone, G., Teodoriu, C., et al., 2013. HPHT viscosities measurements of mixtures of methane/nitrogen and methane/carbon dioxide. J. Nat. Gas Sci. Eng. 12, 43–55. https://doi.org/10.1016/j.jngse.2013.01.005.

De la Porte, J.J., Kossack, C.A., 2014. A liquid phase viscosity–temperature model for long-chain n-alkanes up to $C_{64}H_{130}$ based on the Free Volume Theory. Fuel 136, 156–164. https://doi.org/10.1016/j.fuel.2014.07.016.

Dehlouz, A., Privat, R., Galliero, G., 2021. Revisiting the entropy-scaling concept for shear-viscosity estimation from cubic and SAFT equations of state: application to pure fluids in gas, liquid and supercritical states. Ind. Eng. Chem. Res. 60 (34), 12719–12739. https://doi.org/10.1021/acs.iecr.1c01386.

Diller, D.E., 1982. Measurements of the viscosity of compressed gaseous and liquid nitrogen+methane mixtures. Int. J. Thermophys. 3 (3), 237–249. https://doi.org/10.1007/BF00503319.

Diller, D.E., 1984. Measurements of the viscosity of compressed gaseous and liquid methane+ethane mixtures. J. Chem. Eng. Data 29 (2), 215–221. https://doi.org/10.1021/je00036a035.

Diller, D.E., Van Poolen, L.J., Dos Santos, F.V., 1988. Measurements of the viscosities of compressed fluid and liquid carbon dioxide+ethane mixtures. J. Chem. Eng. Data 33 (4), 460–464. https://doi.org/10.1021/je00054a020.

Elsharkawy, A.M., Hassan, S.A., Hashim, Y.S.K., 2003. New compositional models for calculating the viscosity of crude oils. Ind. Eng. Chem. Res. 42 (17), 4132–4142. https://doi.org/10.1021/ie0300631.

Fan, T.B., Wang, L.S., 2006. A viscosity model based on Peng–Robinson equation of state for light hydrocarbon liquids and gases. Fluid Phase Equil. 247 (1–2), 59–69. https://doi.org/10.1016/j.fluid.2006.06.008.

Fouad, W.A., Vega, L.F., 2018. Transport properties of HFC and HFO based refrigerants using an excess entropy scaling approach. J. Supercrit. Fluids 131, 106–116. https://doi.org/10.1016/j.supflu.2017.09.006.

Giddings, J.G., Kao, J.T., Kobayashi, R., 1966. Development of a high-pressure capillary-tube viscometer and its application to methane, propane, and their mixtures in the gaseous and liquid regions. J. Chem. Phys. 45 (2), 578–586. https://doi.org/10.1063/1.1727611.

Gomez-Osorio, M.A., Browne, R.A., Carvajal Diaz, M., et al., 2016. Density measurements for ethane, carbon dioxide, and methane+nitrogen mixtures from 300 to 470 K up to 137 MPa using a vibrating tube densimeter. J. Chem. Eng. Data 61 (8), 2791–2798. https://doi.org/10.1021/acs.jced.6b00138.

Gonçalves, C.I., Silva, G.M., Ndiaye, P.M., et al., 2021. Helmholtz scaling: an alternative approach to calculate viscosity with the PCP-saft equation of state. Ind. Eng. Chem. Res. 60 (25), 9231–9245. https://doi.org/10.1021/acs.iecr.1c00837.

Gross, J., Sadowski, G., 2001. Perturbed-chain SAFT: an equation of state based on a perturbation theory for chain molecules. Ind. Eng. Chem. Res. 40 (4), 1244–1260. https://doi.org/10.1021/ie0003887.

Guo, J.J., Xiong, W., Hu, Q.Y., et al., 2022. Stability analysis and two-phase flash calculation for confined fluids in nanopores using a novel phase equilibrium calculation framework. Ind. Eng. Chem. Res. 61 (5), 2306–2322. https://doi.org/10.1021/acs.iecr.1c03587.

Haghbakhsh, R., Parvaneh, K., Raeissi, S., et al., 2018. A general viscosity model for deep eutectic solvents: the free volume theory coupled with association equations of state. Fluid Phase Equil. 470, 193–202. https://doi.org/10.1016/j.fluid.2017.08.024.

Jarrahian, A., Aghel, B., Heidaryan, E., 2015. On the viscosity of natural gas. Fuel 150, 609–618. https://doi.org/10.1016/j.fuel.2015.02.049.

Jaubert, J.N., Le Guennec, Y., Piña Martinez, A., et al., 2020. Benchmark database containing binary-system-high-quality-certified data for cross-comparing thermodynamic models and assessing their accuracy. Ind. Eng. Chem. Res. 59 (33), 14981–15027. https://doi.org/10.1021/acs.iecr.0c01734.

Jaubert, J.N., Privat, R., 2021. SAFT and cubic EoS: type of deviation from ideality naturally predicted in the absence of BIPs. Application to the modelling of athermal mixtures. Fluid Phase Equil. 533, 112924. https://doi.org/10.1016/j.fluid.2020.112924.

Kashefi, K., Chapoy, A., Bell, K., et al., 2013. Viscosity of binary and multicomponent hydrocarbon fluids at high pressure and high temperature conditions: measurements and predictions. J. Petrol. Sci. Eng. 112, 153–160. https://doi.org/10.1016/j.petrol.2013.10.021.

Khemka, Y., Abutaqiya, M.I., Chapman, W.G., et al., 2020. Viscosity modeling of light crude oils under gas injection using one-parameter friction theory. Ind. Eng. Chem. Res. 59 (50), 21994–22006. https://doi.org/10.1021/acs.iecr.0c04712.

Khemka, Y., Abutaqiya, M.I., Sisco, C.J., et al., 2021. Accurate prediction of the viscosity of light crude oils using one-parameter friction theory: effect of crude oil characterization methods and property correlations. Fuel 283, 118926. https://doi.org/10.1016/j.fuel.2020.118926.

Lee, A.L., Gonzalez, M.H., Eakin, B.E., 1966. The viscosity of natural gases. J. Petrol. Technol. 18 (8), 997–1000. https://doi.org/10.2118/1340-PA.

Lindeloff, N., Pedersen, K.S., Ronningsen, H.P., et al., 2003. The corresponding states viscosity model applied to heavy oil systems. In: Canadian International Petroleum Conference. OnePetro. https://doi.org/10.2118/2003-150.

Liu, H., Wu, Y., Guo, P., et al., 2019. Compressibility factor measurement and simulation of five high-temperature ultra-high-pressure dry and wet gases. Fluid Phase Equil. 500, 112256. https://doi.org/10.1016/j.fluid.2019.112256.

Llovell, F., Marcos, R.M., Vega, L.F., 2013. Free-volume theory coupled with soft-SAFT for viscosity calculations: comparison with molecular simulation and experimental data. J. Phys. Chem. B 117 (27), 8159–8171. https://doi.org/10.1021/jp401307t.

Locke, C.R., Stanwix, P.L., Hughes, T.J., et al., 2015. Viscosity of {xCO_2+(1−x)CH_4} with x=0.5174 for temperatures between (229 and 348) K and pressures between (1 and 32) MPa. J. Chem. Therm. 87, 162–167. https://doi.org/10.1016/j.jct.2015.03.007.

Lohrenz, J., Bray, B.G., Clark, C.R., 1964. Calculating viscosities of reservoir fluids from their compositions. J. Petrol. Technol. 16 (10), 1171–1176. https://doi.org/10.2118/915-PA.

Lötgering-Lin, O., Gross, J., 2015. Group contribution method for viscosities based on entropy scaling using the perturbed-chain polar statistical associating fluid theory. Ind. Eng. Chem. Res. 54 (32), 7942–7952. https://doi.org/10.1021/acs.iecr.5b01698.

Lötgering-Lin, O., Fischer, M., Hopp, M., et al., 2018. Pure substance and mixture viscosities based on entropy scaling and an analytic equation of state. Ind. Eng. Chem. Res. 57 (11), 4095–4114. https://doi.org/10.1021/acs.iecr.7b04871.

Mairhofer, J., 2021. A residual entropy scaling approach for viscosity based on the GERG-2008 equation of state. Ind. Eng. Chem. Res. 60 (6), 2652–2662. https://doi.org/10.1021/acs.iecr.7b04871.

Mohagheghian, E., Hassanzadeh, H., Chen, Z., 2020. Evaluation of shale-gas-phase behavior under nanoconfinement in multimechanistic flow. Ind. Eng. Chem. Res. 59 (33), 15048–15057. https://doi.org/10.1021/acs.iecr.0c02615.

Motahhari, H., Satyro, M.A., Yarranton, H.W., 2012. Viscosity prediction for natural gas processing applications. Fluid Phase Equil. 322, 56–65. https://doi.org/

10.1016/j.fluid.2012.03.006.
Nazeri, M., Chapoy, A., Burgass, R., et al., 2018. Viscosity of CO_2-rich mixtures from 243 K to 423 K at pressures up to 155 MPa: new experimental viscosity data and modelling. J. Chem. Therm. 118, 100–114. https://doi.org/10.1016/j.jct.2017.11.005.
Neufeld, P.D., Janzen, A.R., Aziz, R., 1972. Empirical equations to calculate 16 of the transport collision integrals Ω(l,s)* for the Lennard-Jones (12–6) potential. J. Chem. Phys. 57 (3), 1100–1102. https://doi.org/10.1063/1.1678363.
Nikolaidis, I.K., Privat, R., Jaubert, J.N., et al., 2021. Assessment of the perturbed chain-statistical associating fluid theory equation of state against a benchmark database of high-quality binary-system data. Ind. Eng. Chem. Res. 60 (24), 8935–8946. https://doi.org/10.1021/acs.iecr.1c01234.
Novak, L.T., 2011a. Self-diffusion coefficient and viscosity in fluids. Int. J. Chem. React. Eng. 9 (1), 1–25. https://doi.org/10.1515/1542-6580.2640.
Novak, L.T., 2011b. Fluid viscosity-residual entropy correlation. Int. J. Chem. React. Eng. 9 (1), 1–27. https://doi.org/10.2202/1542-6580.2839.
Parvaneh, K., Haghbakhsh, R., Rahimpour, M.R., 2016. High pressure viscosity modeling of pure alcohols based on classical and advanced equations of state. J. Taiwan Inst. Chem. Eng. 58, 57–70. https://doi.org/10.1016/j.jtice.2015.05.040.
Pedersen, K.S., Fredenslund, A., Christensen, P.L., et al., 1984. Viscosity of crude oils. Chem. Eng. Sci. 39 (6), 1011–1016. https://doi.org/10.1016/0009-2509(84)87009-8.
Pedersen, K.S., Fredenslund, A.A.G.E., 1987. An improved corresponding states model for the prediction of oil and gas viscosities and thermal conductivities. Chem. Eng. Sci. 42 (1), 182–186. https://doi.org/10.1016/0009-2509(87)80225-7.
Quiñones-Cisneros, S.E., Zéberg-Mikkelsen, C.K., Stenby, E.H., 2001. One parameter friction theory models for viscosity. Fluid Phase Equil. 178 (1–2), 1–16. https://doi.org/10.1016/S0378-3812(00)00474-X.
Quiñones-Cisneros, S.E., Zéberg-Mikkelsen, C.K., Baylaucq, A., et al., 2004. Viscosity modeling and prediction of reservoir fluids: from natural gas to heavy oils. Int. J. Thermophys. 25 (5), 1353–1366. https://doi.org/10.1007/s10765-004-5743-z.
Quiñones-Cisneros, S.E., Zéberg-Mikkelsen, C.K., Fernández, J., et al., 2006. General friction theory viscosity model for the PC-SAFT equation of state. AIChE J. 52 (4), 1600–1610. https://doi.org/10.1002/aic.10755.
Quiñones-Cisneros, S.E., Schmidt, K.A., Giri, B.R., et al., 2012. Reference correlation for the viscosity surface of hydrogen sulfide. J. Chem. Eng. Data 57 (11), 3014–3018. https://doi.org/10.1021/je300601h.
Regueira, T., Pantelide, G., Yan, W., et al., 2016. Density and phase equilibrium of the binary system methane+n-decane under high temperatures and pressures. Fluid Phase Equil. 428, 48–61. https://doi.org/10.1016/j.fluid.2016.08.004.
Rokni, H.B., Moore, J.D., Gupta, A., 2019a. Entropy scaling based viscosity predictions for hydrocarbon mixtures and diesel fuels up to extreme conditions. Fuel 241, 1203–1213. https://doi.org/10.1016/j.fuel.2018.12.043.
Rokni, H.B., Moore, J.D., Gupta, A., 2019b. General method for prediction of thermal conductivity for well-characterized hydrocarbon mixtures and fuels up to extreme conditions using entropy scaling. Fuel 245, 594–604. https://doi.org/10.1016/j.fuel.2019.02.044.
Rokni, H.B., Moore, J.D., Gavaises, M., 2021. Entropy-scaling based pseudo-component viscosity and thermal conductivity models for hydrocarbon mixtures and fuels containing iso-alkanes and two-ring saturates. Fuel 283, 118877. https://doi.org/10.1016/j.fuel.2020.118877.
Satyro, M.A., Yarranton, H.W., 2010. Expanded fluid-based viscosity correlation for hydrocarbons using an equation of state. Fluid Phase Equil. 298 (1), 1–11. https://doi.org/10.1016/j.fluid.2010.06.023.
Schmidt, K.A., Quinones-Cisneros, S.E., Carroll, J.J., et al., 2008. Hydrogen sulfide viscosity modeling. Energy Fuel. 22 (5), 3424–3434. https://doi.org/10.1021/ef700701h.
Stephan, K., 1979. Viscosity of Dense Fluids. Springer, Boston, MA.
Tan, S.P., Adidharma, H., Towler, B.F., et al., 2005. Friction theory and free-volume theory coupled with statistical associating fluid theory for estimating the viscosity of pure *n*-alkanes. Ind. Eng. Chem. Res. 44 (22), 8409–8418. https://doi.org/10.1021/ie050723x.
Tian, Y., Xiong, Y., Wang, L., et al., 2019. A compositional model for gas injection IOR/EOR in tight oil reservoirs under coupled nanopore confinement and geomechanics effects. J. Nat. Gas Sci. Eng. 71, 102973. https://doi.org/10.1016/j.jngse.2019.102973.
Wei, C., Cheng, S., Wang, Y., et al., 2021. Practical pressure-transient analysis solutions for a well intercepted by finite conductivity vertical fracture in naturally fractured reservoirs. J. Petrol. Sci. Eng. 204, 108768. https://doi.org/10.1016/j.petrol.2021.108768.
Wei, C., Liu, Y., Deng, Y., et al., 2022. Temperature transient analysis of naturally fractured geothermal reservoirs. SPE J. 1–23. https://doi.org/10.2118/205862-PA.
Wu, X., Li, C., Jia, W., 2014. An improved viscosity model based on Peng–Robinson equation of state for light hydrocarbon liquids and gases. Fluid Phase Equil. 380, 147–151. https://doi.org/10.1016/j.fluid.2014.08.001.
Xiong, W., Bian, X.Q., Liu, Y.B., 2020. Phase equilibrium modeling for methane solubility in aqueous sodium chloride solutions using an association equation of state. Fluid Phase Equil. 506, 112416. https://doi.org/10.1016/j.fluid.2019.112416.
Xiong, W., Zhang, L.H., Zhao, Y.L., et al., 2021a. A generalized equation of state for associating fluids in nanopores: application to CO_2-H_2O, CH_4-H_2O, CO_2-CH_4, and CO_2-CH_4-H_2O systems and implication for extracting dissolved CH_4 by CO_2 injection. Chem. Eng. Sci. 229, 116034. https://doi.org/10.1016/j.ces.2020.116034.
Xiong, W., Zhao, Y.L., Qin, J.H., et al., 2021b. Phase equilibrium modeling for confined fluids in nanopores using an association equation of state. J. Supercrit. Fluids 169, 105118. https://doi.org/10.1016/j.supflu.2020.105118.
Yarranton, H.W., Satyro, M.A., 2009. Expanded fluid-based viscosity correlation for hydrocarbons. Ind. Eng. Chem. Res. 48 (7), 3640–3648. https://doi.org/10.1021/ie801698h.
Zéberg-Mikkelsen, C.K., 2001. Viscosity Study of Hydrocarbon Fluids at Reservoir Conditions: Modeling and Measurements. Technical University of Denmark, Lyngby.
Zéberg-Mikkelsen, C.K., Quiñones-Cisneros, S.E., Stenby, E.H., 2002. Viscosity prediction of natural gas using the friction theory. Int. J. Thermophys. 23 (2), 437–454. https://doi.org/10.1023/A:1015126022584.
Zhang, T., Javadpour, F., Yin, Y., et al., 2020. Upscaling water flow in composite nanoporous shale matrix using lattice Boltzmann method. Water Resour. Res. 56 (4), e2019WR026007. https://doi.org/10.1029/2019WR026007.
Zhang, T., Javadpour, F., Li, J., et al., 2021. Pore-scale perspective of gas/water two-phase flow in shale. SPE J. 26 (2), 828–846. https://doi.org/10.2118/205019-PA.
Zhao, Y.L., Xiong, W., Zhang, L.H., et al., 2021. Phase equilibrium modeling for interfacial tension of confined fluids in nanopores using an association equation of state. J. Supercrit. Fluids 176, 105322. https://doi.org/10.1016/j.supflu.2021.105322.